THE JOURNAL OF PHYSICAL CHEMISTRY Letters

Letter

Cite This: J. Phys. Chem. Lett. 2019, 10, 4752−4757

pubs.acs.org/JPCL

Enhanced Dissociation of Hot Excitons with an Applied Electric Field under Low-Power Photoexcitation in Two-Dimensional Perovskite Quantum Wells

Vidya Kattoor,[†,‡] Kamlesh Awasthi,[†] Efat Jokar,[†] Eric Wei-Guang Diau,[*,†,§] and Nobuhiro Ohta[*,†,§]

[†]Department of Applied Chemistry and Institute of Molecular Science, National Chiao Tung University, 1001 Ta-Hsueh Road, Hsinchu 30010, Taiwan

[‡]Sustainable Chemical Science and Technology (SCST), Taiwan International Graduate Program (TIGP), Academia Sinica, Nankang, Taipei 115, Taiwan

[§]Center for Emergent Functional Matter Science, National Chiao Tung University, 1001 Ta-Hsueh Road, Hsinchu 30010, Taiwan

Supporting Information

ABSTRACT: The dependence of photoluminescence (PL) on excitation power and the effect of an external electric field have been studied for a two-dimensional (2D) perovskite $(C_4H_9NH_3)_2PbI_4$ thin-film sample. The efficiency of dissociation of hot excitons to produce free carriers was enhanced with a small excitation power because the relaxation of hot excitons to cold emissive excitons was slow, indicating that the thermal energies of hot carriers can be utilized in solar cells under weak photoirradiation. The dissociation was notably enhanced with an applied electric field, resulting in efficient field-induced quenching of the PL. The present results shed light on an application of 2D perovskite materials to photovoltaic (PV) devices with dim radiation, e.g., for indoor PV applications; the concept of electric field-assisted solar cells might be applicable to next-generation solar cells.

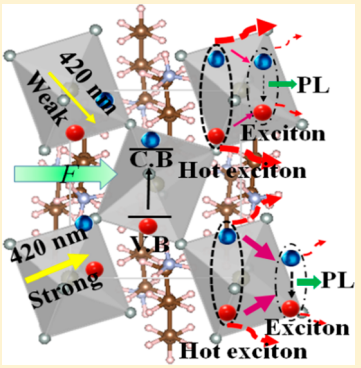

Two-dimensional (2D) hybrid organo−inorganic halide perovskites are emerging as promising classes of materials for photovoltaics (PV) and optoelectronics with both fundamental and technological interests.[1−4] The quantum and dielectric confinement effects in 2D perovskites typically induce a large exciton binding energy and anisotropic charge transport, which undergo significant radiative recombination in the 2D bulk crystals.[3,5] Despite the varied research on photoluminescence (PL) of 2D perovskites, little has been identified about the dynamics of the excited state in the presence of an external electric field (F). The measurements of electroabsorption (E-A) and electrophotoluminescence (E-PL) spectra, i.e., field-induced change in absorption and PL spectra, respectively, are useful for solving those problems.[6−8] Such E-A and E-PL spectra have been reported for thin films of the 2D perovskite butylammonium lead iodide ($(C_4H_9NH_3)_2PbI_4$) (N1).[9] Our measurements of PL indicated a strong dependence of the PL characteristics on the excitation power in both the absence and presence of an electric field. On the basis of the present observations of that dependence on excitation power of quantum yields and decays of PL, we report the intermediate dynamics of hot excitons and the corresponding effect of an electric field. The present work on the dependence of the PL on excitation power enhances our understanding of N1 for application to solar cells under dim light[10−12] or in the presence of an electric field.

Experimental details appear in the Supporting Information. Homogeneous N1 films (thickness ≈ 130 nm) were prepared on a fluorine-doped tin-oxide (FTO)-coated glass substrate with hot casting. Steady-state PL (I^0_{PL}) and E-PL intensity (I^F_{PL}) were measured simultaneously with varied magnitudes of photon density of excitation light (PDEL) in the range 0.08−0.86 mW cm^{-2} at 295 K, which corresponds to 1.69 × 10^{14} to 1.82 × 10^{15} photons s^{-1} cm^{-2} at 420 nm. The E-PL spectra recorded at field strength 0.4 MV cm^{-1} are shown in Figure 1, together with the PL spectra. The excitonic transition was centered at 524 nm in the PL spectra; a minimum intensity appeared at 523 nm in the E-PL spectra. The near-band-edge emission at 524 nm might have several origins such as a recombination of free excitons, free carriers, or bound excitons. The underlying mechanism of recombination becomes identifiable from the dependence of the PL on excitation power. In a semiconductor with a direct band gap, the PL intensity "I" generally depends on the power of the excitation light "L" as $I \propto L^k$; k denotes the power index with $1 < k < 2$ for bound exciton emission and $k < 1$ for a free-to-bound transition.[13] If the k value is near 2 or 1, a recombination of free charges or free excitons, respectively, becomes more pronounced. As Figure 1b shows, the intensity

Received: June 18, 2019
Accepted: August 4, 2019
Published: August 4, 2019

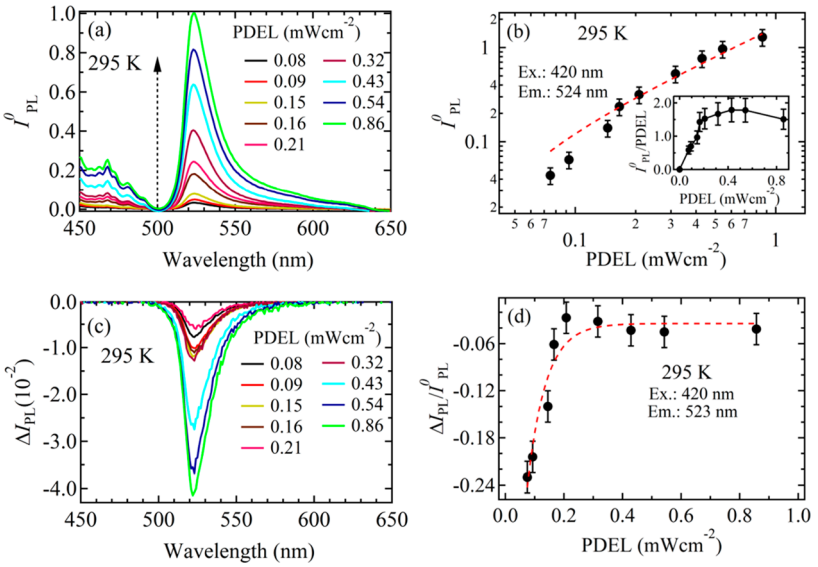

Figure 1. PL and E-PL characterization of N1 film (excitation at 420 nm, 295 K). (a) PDEL-dependent PL spectra, where the maximum intensity in the spectrum observed with 0.86 mW cm^{-2} is normalized to unity. (b) Plots of integrated PL intensity as a function of PDEL on a logarithmic scale; a red dotted line shows the power-law dependence with $k = 1$. (c) PDEL-dependent steady-state E-PL spectra, and (d) plots of $\Delta I_{PL}/I^0_{PL}$ as a function of PDEL. Plots of I^0_{PL}/PDEL as a function of PDEL in a linear scale are shown also in the inset of panel b. The broken red line in panel d is for visual guidance.

at 524 nm exhibits a power-law dependence with k near 1.0 at a large PDEL, indicating that with a large PDEL this sharp emission is due to recombination of free excitons. The result $k \approx 1$ matches those reported for excitons in 2D perovskites.[14,15] When the PDEL was small, the power dependence deviated much from that with $k = 1$. As is mentioned below, the deviation arose from the small yield of the emissive exciton state populated from hot excitons produced following photoexcitation. With increasing PDEL, the yield of PL increased and became saturated at large PDEL with $k = 1$. Despite the variation of the PL quantum yield, the position and shape of the PL spectra were unaffected by a variation of the PDEL (Figure S1), which indicates the absence of a recombination of free carriers.[16]

Figure 1c shows that the E-PL intensity was negative for all PDEL, which clearly indicates that the quantum yield (QY) of PL decreased in the presence of an electric field. The PL quenching exceeded 20% with a small PDEL, i.e., the field-induced variation of the PL intensity relative to the intensity at zero field ($\Delta I_{PL}/I^0_{PL}$) was more than 0.2 with field strength 0.4 MV cm^{-2} and PDEL 0.08 mW cm^{-2}, which monotonically decreased with increasing PDEL and saturated about 0.2 mW cm^{-2} with $\Delta I_{PL}/I^0_{PL} \approx 0.05$ (Figure 1d). ΔI_{PL} hence depended strongly on the PDEL: a small PDEL had a strong influence on the effect of an electric field on the quantum yield; the influence decreased with increasing PDEL. CdSe/CdS nanocrystal tetrapods, which are interesting blocks for an excitonic circuit, also show a field-induced quenching of the PL that depends similarly on the PDEL; a logarithmic decrease of PL with increasing PDEL to a uniform saturation was reported.[17]

To elucidate the origin of the dependence of the QY on the PDEL of 2D perovskite N1 and its effect on the electric field, we measured time-resolved decays of PL in the absence and presence of an electric field, with excitation at 420 nm and PL monitored at 524 nm. The PL decay profile depended on the PDEL even at zero field, as Figure 2 shows. A rise and decay profile was observed with PDEL of 3.3 nJ cm^{-2} pulse^{-1}; the

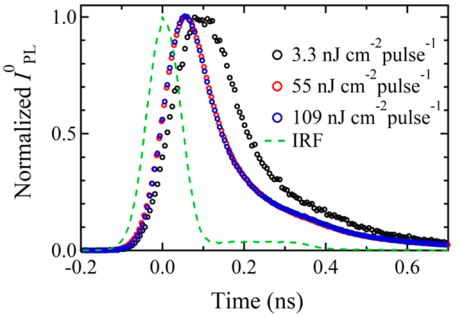

Figure 2. PL decay profiles observed with different PDEL and time profile of the scattered light of the excitation light (IRF).

rise time was estimated to be 63 ps. With PDEL of 55 nJ cm^{-2} pulse^{-1}, the rise was too rapid to detect with the available time resolution. The decay profiles were simulated on assuming a triexponential decay for decay components. The results appear in the Supporting Information (Figure S2 and Table S1). The average lifetime (τ_{ave}) was smaller with a small PDEL: τ_{ave} was 82 ps at 3.3 nJ cm^{-2} pulse^{-1} and about 100 ps at 110 nJ cm^{-2} pulse^{-1}. The decrease of τ_{ave} arose mainly from the decreased pre-exponential factor of the most rapid decay component, of which the lifetime was 72−77 ps, with increasing PDEL, as Table S1 shows.

The effects of the electric field on the PL decay profile observed with varied PDEL are shown in Figure 3, in which the difference between two decay profiles observed with field 0.4 MV cm^{-1} and zero field, (ON − OFF), and the ratio, (ON/OFF), are presented. The negative value of the difference indicates the field-induced quenching, consistent with the steady-state E-PL measurements; the ratio is less than unity at time $t = 0$, and this ratio decreases as a function of t (Figure 3d), indicating a decreased population of the emitting state as well as a decreased PL lifetime in the presence of the field. As mentioned in the Supporting Information, PL decay profiles were obtained simultaneously by dividing the memory

DOI: 10.1021/acs.jpclett.9b01759
J. Phys. Chem. Lett. 2019, 10, 4752−4757

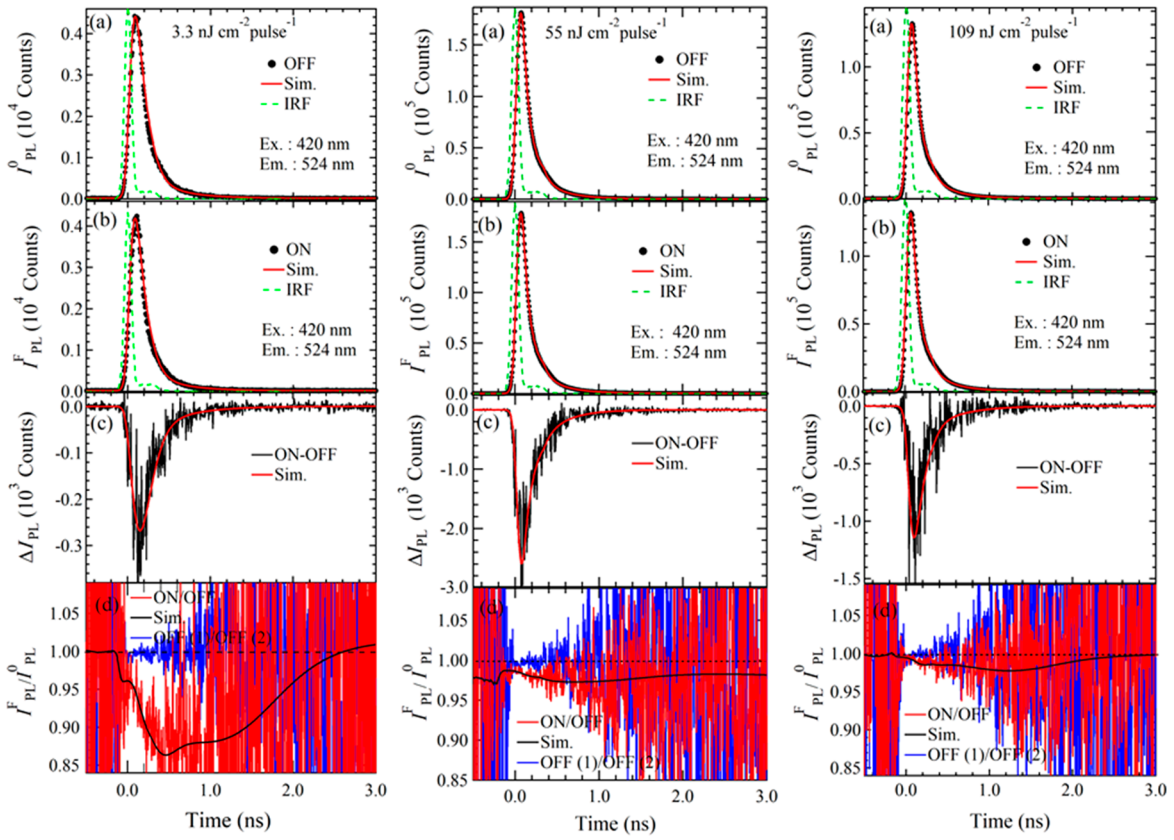

Figure 3. Effects of an electric field on PL decay profiles of an N1 film with varied PDEL as indicated. (a) Decay profiles observed at zero field I^0_{PL} (OFF), (b) with field I^F_{PL} = 0.4 MV cm^{-1} (ON), (c) difference ΔI_{PL} (ON-OFF), (d) ratio I^F_{PL}/I^0_{PL} (red, ON/OFF). The blue line in panel d gives the ratio of two decay profiles at zero field accumulated in different segments at the same experiment (see text and the Supporting Information for details). Simulated curves and the IRF are also shown in the figures.

channels of multichannel analyzer (MCA) into four segments.[18] The applied voltage had a repetition of rectangular waves of positive, zero, negative, and zero bias in turn. The switching of MCA is synchronized with a modulated applied voltage, and four decay profiles which correspond to the applied electric field of +0.4, 0, −0.4, 0 MVcm^{-1}, respectively, were obtained simultaneously. The decay "ON" in Figure 3 was obtained by adding two decay profiles which correspond to +0.4 and −0.4 MVcm^{-1}, respectively. Then, the decay "ON" can be compared with the steady-state E-PL spectra shown in Figure 1 because these E-PL spectra were obtained at the second harmonic of the modulation frequency of applied ac voltage. The ratio of two decay profiles at zero field which were accumulated in different segments simultaneously, i.e., OFF(1)/OFF(2), which is also shown in Figure 3, is essentially constant in the whole time region, in contrast with ON/OFF. Note that the decay "OFF" in Figure 3 was obtained from OFF(1) + OFF(2). The clear difference between the plots ON/OFF and OFF(1)/OFF(2) in Figure 3 shows that the field effect on PL decay profiles is reliable.

In the N1 sample having a volume of 1.3 × 10^{-5} cm^3, i.e., 130 nm (sample thickness) × 1 cm^2, where laser light was assumed to be irradiated, the total number of N1 molecules included in this volume may be estimated to be ∼2.3 × 10^{16}, with interplanar distance of 13.83 Å and thickness of inorganic layer of 6.41 Å in the N1 crystal.[1,19] The excitation laser pulse having a power density of 3.3, 55, and 109 nJ cm^{-2} pulse^{-1} at 420 nm correspond to ∼7.0 × 10^9, ∼1.2 × 10^{11}, and ∼2.3 × 10^{11} photon numbers cm^{-2} for each pulse. The absorbance of the sample at 420 nm was about 0.25, that is, 44% of the incident light was absorbed. Then, the number of photons absorbed by N1, which corresponds to the number of excited species of N1, is estimated to be 3.1 × 10^9, 5.3 × 10^{10}, and 1.1 × 10^{11} per cm^2. Then, the ratio of the number of excited species of N1 relative to the total number of N1 is estimated to be ∼1.3 × 10^{-7}, ∼2.3 × 10^{-6}, and ∼4.8 × 10^{-6}, respectively. Thus, the density of the excited species of N1 is not so large in any power density, and it is surprising that strong PDEL dependence in PL is observed with these quantities of excited species of N1.

PL decay profiles observed in the presence of the field were simulated in a manner similar to the decay profiles at zero field (Figure S2); the profiles of difference and ratio were also simulated (Figure 3). The results of the lifetime and the pre-exponential factor of each component at 0.4 MV cm^{-1} are shown in Table S1 with the average lifetime and the sum of the pre-exponential factors. The rise time observed in the decay with small PDEL, i.e., 3.3 nJ cm^2 pulse^{-1}, decreased from 63 to 60 ps with 0.4 MV cm^{-1}. The sum of the pre-exponential factors of the decay components decreased by about 5%, 1.2%, and 0.4% with F = 0.4 MV cm^{-1} and PDEL = 3.3, 55, and109 nJ cm^{-2} pulse^{-1}, respectively (Table S1), indicating that the population of the emitting state of the PL decreases in the presence of an electric field and that the magnitude of the field-induced decrease of population of the PL- emitting state became larger with decreasing PDEL. Both the average lifetime and the lifetime of the most rapid decay component decreased on the applied electric field (Table S1). In the steady-state PL

DOI: 10.1021/acs.jpclett.9b01759
J. Phys. Chem. Lett. 2019, 10, 4752−4757

and E-PL spectra, emissions in the whole time region were monitored. In Figure 3, on the other hand, decay profiles are shown only in the time scale of 0−3 ns. However, the amount of the field-induced quenching of PL in the steady-state experiments and in the time-resolved experiments is in the same order. Therefore, it is concluded that free-exciton recombination plays an important role in the present results at room temperature.

The present experimental results are summarized as follows: (1) The PL quantum yield increased with increasing PDEL and became saturated at large PDEL; the power-law dependence of the PL intensity with k near 1 was observed only with a large PDEL. (2) Even with varied PDEL, there was neither spectral shift nor significant change of the spectral shape. (3) A rise and decay profile was observed only with small PDEL. (4) The PL was quenched on application of an electric field. (5) The efficiency of the field-induced quenching of PL increased with decreasing PDEL in the region of small power, although the efficiency was nearly the same under conditions of large power. (6) The rise time observed with a small PDEL became faster in the presence of an electric field. (7) The pre-exponential factor of the decay component decreased in the presence of an electric field; the magnitude of the decrease increased with decreasing PDEL. (8) The average lifetime of the PL decay profile decreased on application of an electric field.

These results become explicable with the scheme shown in Figure 4. Following photoexcitation from the valence band

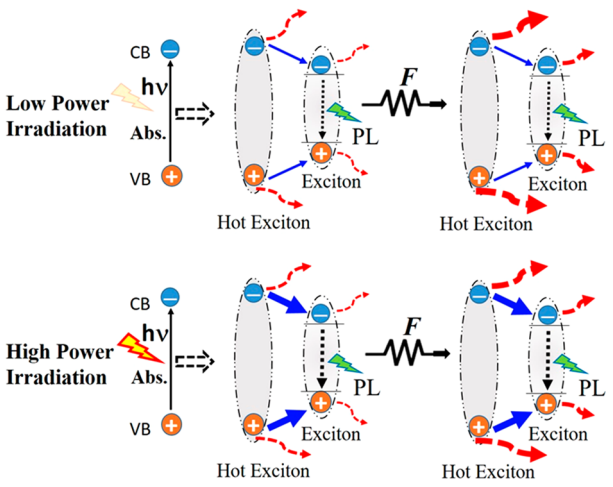

Figure 4. Relaxation pathways and the change in dynamics after application of external electric field (F). Blue solid arrows and red broken lines show relaxation of hot exciton to emissive exciton and dissociation process of hot exciton and emissive exciton, respectively. The thickness of the blue and red arrows corresponds to the rate of the processes.

(VB) to the conduction band (CB) of N1, an intermediate state of an electron−hole pair with excess thermal energy, known as a hot exciton, is produced. The observed PL corresponds to the emission of cold excitons produced after thermal relaxation of hot excitons; the rise in the PL decay profile observed with a small PDEL corresponds to the thermalization of hot excitons. The rate coefficients k_{dis} and k_{rel} represent two competing kinetic processes: the dissociation and thermalization of hot excitons to hot carriers and cold excitons, respectively. With a small PDEL, k_{rel} and k_{dis} are small, resulting in a slow rise of the PL transient profile. With a large PDEL, k_{rel} became large, resulting in the PL transient profile showing only the decay feature due to the pulse-limited rise feature being unobservable. The large PLQY is caused by a large population of the cold emissive excitons. The population efficiency of excitons and the rise time are given by $k_{rel}/(k_{rel} + k_{dis})$ and $1/(k_{rel} + k_{dis})$, respectively.

On application of an electric field, the dissociation of hot excitons was considered to become more rapid, i.e., k_{dis} became larger with the field than without the field. The rise of the PL decay became more rapid; the population of the cold emissive excitons decreased in the presence of that field. The field-induced decrease of the population of the cold emissive excitons and the field-induced PL quenching increased more with a small PDEL than with a large PDEL, as a larger influence of the applied electric field on $k_{rel}/(k_{rel} + k_{dis})$ is expected with a small PDEL than with a large PDEL. The dissociation to produce free carriers occurred also from cold excitons, in competition with the radiative process that gave the PL. This process is also enhanced with the electric field, the same as in the case of the dissociation of hot excitons. The field-induced decrease of the PL lifetime can be interpreted as a field-induced enhancement of the exciton dissociation. With a large PDEL, the quenching of the PL caused by a field-induced enhancement of the dissociation of hot excitons is small, because the population of the cold excitons is less affected by the electric field as rapid thermal relaxation from hot excitons occurs to cold excitons at zero field.

The electron-transfer process and the charge-transfer process are well affected by the applied electric field.[6] Electron transfer from higher vibrational levels of reactant may be more enhanced by the applied electric field, which may result in more enhanced dissociation of the hot exciton than relaxed exciton by application of the electric field. If enhanced annihilation at larger power density plays a significant role as the mechanism of the power dependence of the excitation light on PL, PL intensity as well as its field effect should depend on the square of the magnitude of PDEL because a collision of excited species is necessary. As shown in Figure 1b, however, PL intensity is linearly proportional to PDEL even at higher PDEL, indicating that the observed behavior should be interpreted in terms of unimolecular process.

The above-mentioned results were obtained at room temperature, where only one exciton emission was observed. In contrast with the PL spectra at room temperature, two exciton bands, i.e., H-band (peak 515 nm) and L-band (peak at 495 nm), which come from different phases caused by lattice contraction, and weak trap emission with a peak at 560 nm are observed at low temperatures.[9] Note that H-band corresponds to the exciton band observed at room temperature. PL spectra and E-PL spectra of N1 with different PDEL were observed at 40 K. The results are shown in Figure 5. PDEL dependence of the PL intensity and its field-induced change are similar to those observed at room temperature in the sense that any emission exhibits a power-low dependence with $k \approx 1$ at large power density of excitation light, indicating that these emissions result from a unimolecular process following photoexcitation and that the field-induced quenching becomes larger with decreasing PDEL. The yield of all the emitting states from the hot exciton is considered to decrease with application of the electric field, as in the case at room temperature. However, it is stressed that the magnitude of PDEL dependence of field-induced change in PL intensity at

DOI: 10.1021/acs.jpclett.9b01759
J. Phys. Chem. Lett. 2019, 10, 4752−4757

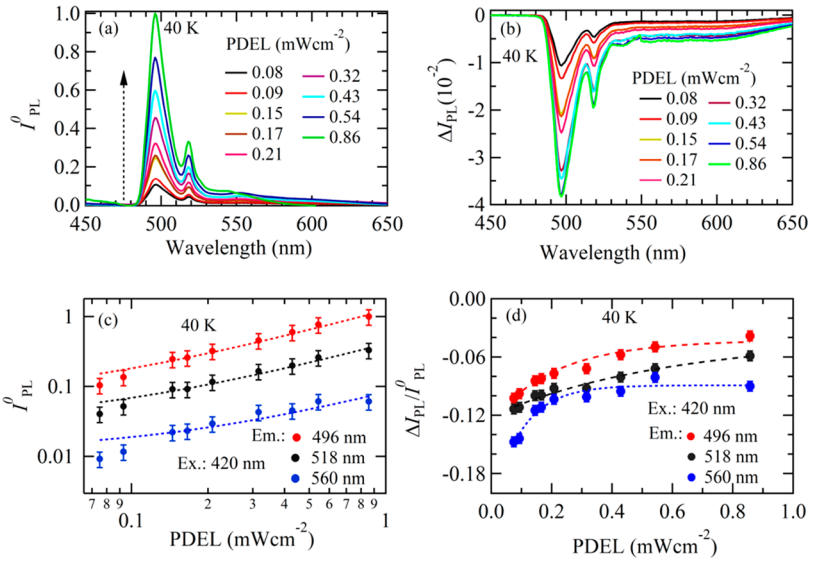

Figure 5. PL and E-PL characterization of an N1 film (excitation at 420 nm, 40 K). (a) PDEL-dependent PL spectra, where the maximum intensity in the spectrum observed with 0.86 mW cm^{-2} is normalized to unity. (b) PDEL-dependent steady-state E-PL spectra. (c) Plots of integrated PL intensity as a function of PDEL on a logarithmic scale. Dotted lines show the power-law dependence with $k = 1$. (d) Plots of $\Delta I_{PL}/I^0_{PL}$ as a function of PDEL. The broken and dotted lines in panel d are for visual guidance.

40 K is much smaller than that at room temperature, implying the thermal effect on the electric field.

In conclusion, the excitation dynamics and emission property of a 2D perovskite $(C_4H_5NH_3)_2PbI_4$ and the effect of an electric field depending on the photon density of excitation light are reported. Under a small PDEL, the thermal relaxation of hot excitons to emissive cold excitons is slow, such that the dissociation of hot excitons to free carriers can occur; this observation indicates that thermal energy might be utilized in perovskite solar cells. An external electric field enhances the dissociation of excitons, resulting in field-induced PL quenching and field-induced decrease of the PL lifetime. With a large PDEL, a large emission quantum yield and a suppression of the field-induced PL quenching are achieved. It is also found that PDEL dependence of PL is observed even at low temperature, but the effect at 40 K is much smaller than that at room temperature. The present results offer a new vision for two-dimensional perovskites to be applied for photovoltaic applications in dim light and the presence of an external electric field.

■ ASSOCIATED CONTENT

Supporting Information

The Supporting Information is available free of charge on the ACS Publications website at DOI: 10.1021/acs.jpclett.9b01759.

Experimental method, excitation light power dependence of PL spectra, simulation of PL decay profile, and fitted parameters to simulate the PL decay profiles (PDF)

■ AUTHOR INFORMATION

Corresponding Authors

*E-mail: diau@mail.nctu.edu.tw.
*E-mail: nohta@nctu.edu.tw.

ORCID

Kamlesh Awasthi: 0000-0001-7852-059X
Eric Wei-Guang Diau: 0000-0001-6113-5679
Nobuhiro Ohta: 0000-0003-4255-6448

Notes

The authors declare no competing financial interest.

■ ACKNOWLEDGMENTS

This work is supported by Ministry of Science and Technology, Taiwan (MOST 107-2113-M-009-005, MOST 108-2113-M-009-002, MOST 108-3017-F-009-004, MOST 107-2119-M-009-001, and MOST 105-2119-M-009-011-MY3) and the Center for Emergent Functional Matter Science of National Chiao Tung University from The Featured Areas Research Center Program within the framework of the Higher Education Sprout Project by the Ministry of Education (MOE) in Taiwan.

■ REFERENCES

(1) Cao, D. H.; Stoumpos, C. C.; Farha, O. K.; Hupp, J. T.; Kanatzidis, M. G. 2D Homologous Perovskites as Light-Absorbing Materials for Solar Cell Applications. *J. Am. Chem. Soc.* **2015**, *137*, 7843−7850.

(2) Smith, I. C.; Hoke, E. T.; Ibarra, D. S.; McGehee, M. D.; Karunadasa, H. I. A Layered Hybrid Perovskite Solar-Cell Absorber with Enhanced Moisture Stability. *Angew. Chem., Int. Ed.* **2014**, *53*, 11232−11235.

(3) Dou, L.; Wong, A. B.; Yu, Y.; Lai, M. L.; Kornienko, N.; Eaton, S. W. A.; Fu, A.; Bischak, C. G.; Ma, J.; Ding, T. N.; et al. Atomically Thin Two-Dimensional Organic-Inorganic Hybrid Perovskites. *Science* **2015**, *349*, 1518−1521.

(4) Dohner, E. R.; Jaffe, A.; Bradshaw, L. R.; Karunadasa, H. I. Intrinsic White-Light Emission from Layered Hybrid Perovskites. *J. Am. Chem. Soc.* **2014**, *136*, 13154−13157.

(5) Era, M.; Morimoto, S.; Tsutsui, T.; Saito, S. Organic-Inorganic Heterostructure Electroluminescent Device using a Layered Perovskite Semiconductor $(C_6H_5C_2H_4NH_3)_2PbI_4$. *Appl. Phys. Lett.* **1994**, *65*, 676−678.

(6) Ohta, N. Electric Field Effects on Photochemical Dynamics in Solid Films. *Bull. Chem. Soc. Jpn.* **2002**, *75*, 1637−1655.

(7) Ohta, N.; Awasthi, K.; Okoshi, K.; Manseki, K.; Miura, H.; Inoue, Y.; Nakamura, K.; Kono, H.; Diau, E. W.-G. Stark

DOI: 10.1021/acs.jpclett.9b01759
J. Phys. Chem. Lett. 2019, 10, 4752−4757

Spectroscopy of Absorption and Emission of Indoline Sensitizers: A Correlation with the Performance of Photovoltaic Cells. *J. Phys. Chem. C* **2016**, *120*, 26206−26216.
(8) Leijtens, T.; Kandada, A. R.; Eperon, G. E.; Grancini, G.; D'Innocenzo, V.; Ball, J. M.; Stranks, S. D.; Snaith, H. J.; Petrozza, A. Modulating the Electron−Hole Interaction in a Hybrid Lead Halide Perovskite with an Electric Field. *J. Am. Chem. Soc.* **2015**, *137*, 15451−15459.
(9) Kattoor, V.; Awasthi, K.; Jokar, E.; Diau, E. W. G.; Ohta, N. Integral Method Analysis of Electroabsorption Spectra and Electrophotoluminescence Study of $(C_4H_9NH_3)_2PbI_4$ Organic−Inorganic Quantum Well. *J. Phys. Chem. C* **2018**, *122*, 26623−26634.
(10) Chen, C. Y.; Chang, J. H.; Chiang, K. M.; Lin, H. L.; Hsiao, S. Y.; Lin, H. W. Perovskite Photovoltaics for Dim-Light Applications. *Adv. Funct. Mater.* **2015**, *25*, 7064−7070.
(11) Juang, S. S.Y.; Lin, P. Y.; Lin, Y. C.; Chen, Y. S.; Shen, P. S.; Guo, Y. L.; Wu, Y. C.; Chen, P. Energy Harvesting Under Dim-Light Condition with Dye-Sensitized and Perovskite Solar Cells. *Front. Chem.* **2019**, *7*, 209.
(12) Raifuku, I.; Ishikawa, Y.; Ito, S.; Uraoka, Y. Characteristics of Perovskite Solar Cells Under Low-illuminance Conditions. *J. Phys. Chem. C* **2016**, *120*, 18986−18990.
(13) Schmidt, T.; Lischka, K.; Zulehner, W. Excitation-Power Dependence of the Near-Band-Edge Photoluminescence of Semiconductors. *Phys. Rev. B: Condens. Matter Mater. Phys.* **1992**, *45*, 8989−8994.
(14) Gan, L.; Fang, J.; Li, Z.; He, H.; Ye, Z. Effects of Organic Cation Length on Exciton Recombination in Two-Dimensional Layered Lead Iodide Hybrid Perovskite Crystals. *J. Phys. Chem. Lett.* **2017**, *8*, 5177−5183.
(15) Gan, L.; He, H.; Li, S.; Li, J.; Ye, Z. Distinctive Excitonic Recombination in Solution-Processed Layered Organic-Inorganic Hybrid Two-Dimensional Perovskites. *J. Mater. Chem. C* **2016**, *4*, 10198−10204.
(16) Smith, M.; Lin, J. Y.; Jiang, H. X.; Khan, M. A. Room Temperature Intrinsic Optical Transition in GaN Epilayers: The Band-to-Band Versus Excitonic Transitions. *Appl. Phys. Lett.* **1997**, *71*, 635−637.
(17) Liu, S.; Borys, N. J.; Huang, J.; Talapin, D. V.; Lupton, J. M. Exciton Storage in CdSe/CdS Tetrapod Semiconductor Nanocrystals: Electric Field Effects on Exciton and Multiexciton States. *Phys. Rev. B: Condens. Matter Mater. Phys.* **2012**, *86*, No. 045303.
(18) Tsushima, M.; Ushizaka, T.; Ohta, N. Time-resolved measurement system of electrofluorescence spectra. *Rev. Sci. Instrum.* **2004**, *75*, 479−485.
(19) Stoumpos, C. C.; Cao, D. H.; Clark, D. J.; Young, J.; Rondinelli, J. M.; Jang, J. I.; Hupp, J. T.; Kanatzidis, M. G. Ruddlesden-Popper Hybrid Lead Iodide Perovskite 2D Homologous Semiconductors. *Chem. Mater.* **2016**, *28*, 2852−2867.

DOI: 10.1021/acs.jpclett.9b01759
J. Phys. Chem. Lett. 2019, 10, 4752−4757